A Clinical-Grade Partially Decellularized Matrix for Tracheal Replacement: Validation In Vitro and In Vivo in a Porcine Model

Lousineh Arakelian, Maëlys Léger, Sabrina Kellouche, Rémy Agniel, Patrick Bruneval, Jean-Marc Allain, Valentino Caputo, Nicolas Gendron, Romane Gozlan, Rezlene Bargui, et al.

ADVANCED BIOLOGY
www.advanced-bio.com

A Clinical-Grade Partially Decellularized Matrix for Tracheal Replacement: Validation In Vitro and In Vivo in a Porcine Model

*Lousineh Arakelian, Maëlys Léger, Sabrina Kellouche, Rémy Agniel, Patrick Bruneval, Jean Marc Allain, Valentino Caputo, Nicolas Gendron, Romane Gozlan, Rezlene Bargui, Augustin Vigouroux, Caroline Sansac, Mohamed Jarraya, Françoise Denoyelle, Jérôme Larghero, and Briac Thierry**

The management of extensive tracheal resection followed by circumferential replacement remains a surgical challenge. Numerous techniques are proposed with mixed results. Partial decellularization of the trachea with the removal of the mucosal and submucosal cells is a promising method, reducing immunogenicity while preserving the biomechanical properties of the final matrix. Despite many research protocols and proofs of concept, no standardized clinical grade protocol is described. Furthermore, local and systemic biointegration mechanisms of decellularized trachea are not well known. Therefore, in a translational research perspective, this work set up a partial tracheal decellularization protocol in line with *Cell and Tissue Products regulations*. Extensive characterization of the final product is performed in vitro and in vivo. The results show that the Partially Decellularized Trachea (PDT) is cell-free in the mucosa and submucosa, while the cartilage structure is preserved, maintaining the biomechanical properties of the trachea. When implanted in the muscle in vivo for 28 days, no systemic inflammation is observed, and locally, the PDT shows an excellent biointegration and vascularization. No signs of graft rejection are observed. These encouraging results confirmed the efficacy of the clinical grade PDT production protocol, which is an important step for future clinical applications.

1. Introduction

Tracheal defects of more than 50% in adults and 30% in children cannot be reconstructed with an end-to-end anastomosis and require circumferential replacement of the resected area.[1] Multiple techniques have been used in clinic with mitigated results. Autologous surgical reconstructions are technically extremely complex.[2–5] Thyrotracheal complex allotransplantations are equally challenging due to the complexity of direct vascular restoration and long-term immunosuppressive therapy.[6,7] Synthetic products are currently not suitable for transplantation.[8] 3D-printed bio-mimetic scaffolds have proven limited biointegration, with limited colonization by patients' cells and neovascularization.[9,10] In terms of biological tissues, aortic allografts show satisfactory biointegration results but aortic malacia requires long-term stenting.[11–13]

L. Arakelian, M. Léger, V. Caputo, R. Gozlan, R. Bargui, A. Vigouroux, J. Larghero, B. Thierry
Inserm
U976, CIC-BT CBT501, Paris F-75475, France
E-mail: briac.thierry@aphp.fr

L. Arakelian, J. Larghero
AP-HP
Hôpital Saint-Louis
Unité de Thérapie Cellulaire
Paris 75010, France

L. Arakelian, M. Léger, R. Gozlan, R. Bargui, A. Vigouroux, F. Denoyelle, J. Larghero, B. Thierry
Université Paris Cité
Paris, France

M. Léger, V. Caputo, F. Denoyelle, B. Thierry
Department of Pediatric Otolaryngology-Head and Neck Surgery
AP-HP
Hôpital Universitaire Necker – Enfants Malades
Paris F-75015, France

The ORCID identification number(s) for the author(s) of this article can be found under https://doi.org/10.1002/adbi.202400208

DOI: 10.1002/adbi.202400208

In this context, decellularization of the trachea is an interesting area of research. This technique makes biological tissues less immunogenic by removing cells, antigens and genomic DNA, while preserving the chemical and biomechanical properties of the extracellular matrix (ECM). Therefore, decellularized tissues can be ideal for biointegration, without graft rejection. Numerous complete decellularization protocols of the trachea have been reported. One of the initial stumbling challenges was the malacia induced by full decellularization, carried out by long and aggressive treatment to remove mucosal cells and chondrocytes. Initial clinical applications have shown poor results.[7,14–16]

In the trachea, epithelial cells are the most immunogenic, while chondrocytes have a low immunogenicity.[7,17–20] Several teams have recently demonstrated in mouse and porcine tracheal models the benefits of partial decellularization, which removes cells only from the mucosa but preserves chondrocytes and the cartilage. Consequently, this trade-off tissue engineering technique makes the matrix less immunogenic, without rendering it malacic.[21,22] Previously published partial decellularization protocols were mainly based on small animal tracheal models, whose size is not compatible with that of humans. As for larger animal models, previously reported partial decellularization methods on pig tracheas showed the presence of remaining cells in the submucosa at the end of their procedure.[21]

Another important step is to evaluate the biocompatibility of the partially decellularized trachea (PDT) in vivo and to understand the mechanisms of biointegration. Like any other decellularized tissue, the PDT needs to be revascularized to become a living tissue and provide an oxygen and nutrient rich environment for host cell colonization.[23] Furthermore, in order to improve this biointegration and tissue regeneration, it is important to understand cellular and molecular mechanisms involved, and the immunological response[24] both at local and systemic levels. Ideally, these mechanisms should be explored in animal models that present a high similarity in terms of immune system with humans. The pig is therefore an ideal candidate for this kind of immunological studies.[25]

Considering the presented elements, and in the aim of a translational research, the objectives of this study were the development of a reliable and reproducible clinical grade partial decellularization protocol using porcine tracheas, implant the PDT in vivo in a porcine model for 28 days and evaluate vascularization and biointegration.

2. Experimental Section

2.1. Porcine Tracheal Harvest

Tracheas from Large White/Landrace pigs weighing between 50 and 70 kg were harvested from freshly sacrificed animals in a professional slaughterhouse of a national research facility (Institut National de Recherche pour l'Agriculture, l'Alimentation et l'Environnement, INRAe, Nouzilly, France). They were transported to our laboratory in physiological serum.

2.2. Partial Decellularization Protocol

Partial decellularization consists of four major steps: decontamination with antibiotics, treatment with a detergent to remove the cells and their contents, rinsing and incubation with activated charcoal cartridge to remove residual detergent and antibiotics, and treatment with DNase to remove the remaining genetic material (**Figure 1**). All these steps were performed under sterile conditions in a laminar flow hood.

2.2.1. Decontamination

Each trachea was rinsed, cleaned of connective tissue and placed in a 500 mL bottle which was used until the end of the process. Tracheas were decontaminated overnight under constant agitation (230 rpm, New Brunswick Innova, 42 R shaker, Eppendorf, Hamburg, Germany) in a solution of antibiotics and antimycotics: 320 mg L^{-1} gentamycin (Panpharma, Luitré, France), 600 mg L^{-1} clindamycin (Pfizer, Paris, France), 500 mg L^{-1} vancomycin (Mylan, Saint-Priest, France), and 100 mg L^{-1} amphotericin B (Bristol-Myers Squibb, Rueil-Malmaison, France) at 24 °C.

2.2.2. Decellularization

This process was performed in order to remove epithelial and submucosal cells. After decontamination, the solution was changed to 1% sodium dodecyl sulfate (SDS; Euromedex, France) prepared in sterile water. The bottles were then placed under orbital agitation (230 rpm) at 24 °C, in a shaking incubator (New Brunswick Innova 42R, Eppendorf France, Montesson). After 24 h, treated tracheas were rinsed with saline for four 20-min cycles

S. Kellouche, R. Agniel
CY Cergy Paris Université
Institut des Matériaux
I-MAT FD4122
Equipe de Recherche sur les Relations Matrice Extracellulaire-Cellules
ERRMECe EA1391, Cergy F-95000, France
P. Bruneval
Department of Pathology
AP-HP
Georges Pompidou European Hospital
Paris F-75015, France
J. M. Allain
LMS
CNRS
Ecole Polytechnique
Institut Polytechnique de Paris
Palaiseau 91120, France
J. M. Allain
Inria
Palaiseau F-91120, France
N. Gendron
Department of Hematology
AP-HP
Georges Pompidou European Hospital
Paris F-75015, France
C. Sansac, M. Jarraya
Banque des Tissus Humains
AP-HP
Hôpital St-Louis, Paris F-75010, France

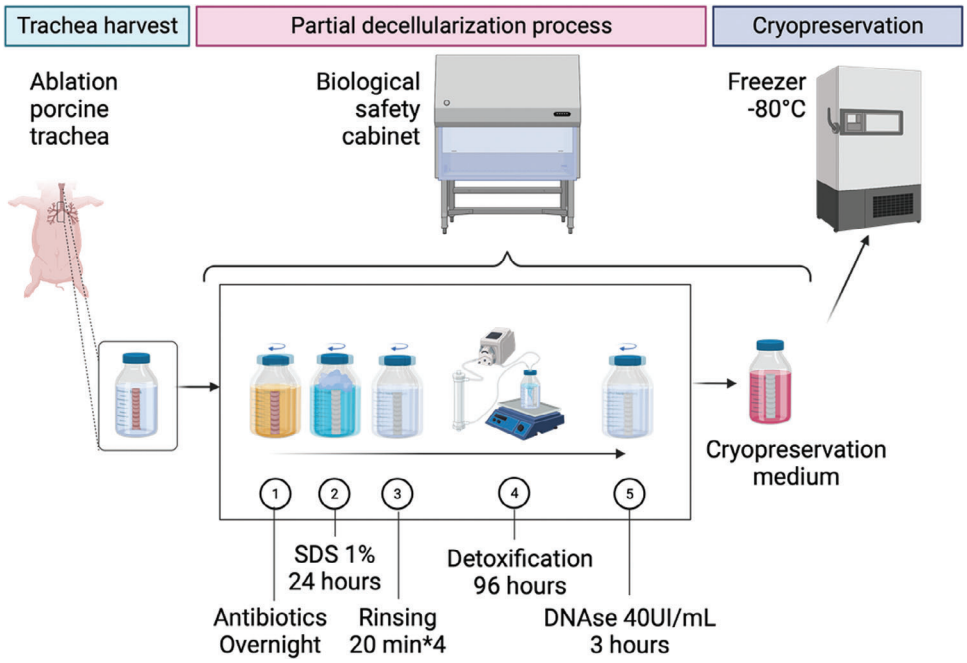

Figure 1. Diagram of decellularization steps from porcine tracheal harvest to cryopreservation. The partial decellularization process is represented. The five steps of decellularization were: decontamination with antibiotics, SDS treatment, rinsing, detoxification with an activated charcoal cartridge and DNAse treatment. All steps were performed in a bottle, under sterile conditions in a laminar flow hood. Cryopreservation enabled long-term storage. SDS: Sodium Dodecyl Sulfate.

at 37 °C. Then, in order to remove residual SDS traces, an activated charcoal cartridge was used. The bottles were filled with sterile water and connected in series to the Adsorba 300C cartridge (Baxter, USA), forming a closed circuit with a peristaltic pump (27 mL min^{-1}). The bottle was placed on a warming magnetic agitator Cimarec (Thermo Fisher Scientific Inc., Waltham, USA) and the solution was continuously filtered for 96 h at 37 °C and 270 rpm. The SDS released from the decellularized trachea was adsorbed by the cellulose-coated activated charcoal (Figure 1).

To remove DNA, the tracheal matrix was incubated for 3 h with DNase 40 UI mL^{-1} (Pulmozyme, Roche, Boulogne-Billancourt, France) at 37 °C under constant orbital agitation (230 rpm) in the shaking incubator (New Brunswick Innova 42R).

2.2.3. Cryopreservation

PDTs were stored in a solution of Roswell Park Memorial Institute Medium (RPMI, Gibco Waltham, MA, U.S.A.) supplemented with 10% DMSO (CryoSure-DMSO, WAK-Chemie Medical GmbH, Germany) and 0.8% Albumin (OctaPharma, Boulogne Billancourt). The descent in temperature was performed in two steps: freezing at −20 °C overnight, then long term preservation at −80 °C.

2.2.4. Sterility

According to the standards of clinical grade human tissue banking, sterility was evaluated on samples of trachea (1) before and (2) after antibiotic and antimycotic treatment, (3) at the end of the decellularization process and (4) after the thawing of cryopreserved PDT. Samples were incubated in Schaedler broth (Biomérieux SA, Craponne, France) for 10 days and then seeded into Chocolate agar + PolyViteX (Biomérieux SA) for aerobic culture, Columbia agar + 5% sheep blood (Biomérieux SA) for anaerobic culture, and Sabouraud chloramphenicol gentamicin agar (Bio-Rad Inc, Hercules, USA) for fungal culture. The bacterial media were incubated at 37 °C for 8 days and the fungal medium at 30 °C for 11 days. In addition, incubated Schaedler for samples (3) and (4) were seeded in aerobic and anaerobic BACT/ALERT – Flasks (Biomérieux, France) for 10 days at 37 °C.

2.3. Histology and Immunostaining

2.3.1. Histology

Native tracheal and PDT segments were fixed in 10% formol and embedded in paraffin. Five-micrometer-thick sections were stained with hematoxylin-eosin-saffron (HES) for general structure and remaining cells, picrosirius red for collagen fibers, orcein for elastic fibers and alcian blue for glycosaminoglycans.

2.3.2. Immunostaining of ECM Components

Deparaffinized histological sections were rinsed with PBS, fixed with 3% paraformaldehyde diluted in PBS (15 min) then rinsed with PBS containing 0.5% bovine serum albumin (BSA). They were permeabilized with 0.1% Triton X100 in PBS for 30 min at room temperature, then rinsed three times with PBS-BSA.

Immunostaining was performed with an association of a primary antibody and a secondary fluorescent antibody. The following primary antibodies were used: Collagen II (ab34712 rabbit polyclonal IgG, Abcam) and Laminin (L9393, rabbit polyclonal IgG, Merck). Histological sections were incubated with the primary antibodies for 2 h at room temperature. After several washes in PBS-BSA, slides were incubated for 1 h at room temperature with Anti-Rabbit Alexa Fluor 568). Cell nuclei were labeled with 4,6-diamino-2-phenylindol dihydrochloride, (DAPI, Sigma Aldrich). The coverslips were mounted in Prolong-Gold antifade reagent (P36930, Invitrogen). Specificity controls were performed by incubating tissues with the secondary antibodies alone, used as negative control. Autofluorescence analysis of histological sections was also performed. Immunofluorescent labeling observations were made under a Zeiss Axio Observer Z1 microscope equipped with an axiocam305 sCMOS camera. The excitation wavelengths used for DAPI, Collagen II and Laminin were 385, and 555 nm, respectively. The lens was EC Plan neofluar x10/0.3.

2.4. DNA Quantification and Qualification in the Mucosa

Native tracheal and PDT samples were collected and the mucosa was separated from the rest of the trachea. Samples of about 30 mg were cut and weighed. They were digested overnight with proteinase K and DNA was extracted using the PureLink Genomic DNA Mini Kit (Invitrogen, USA), according to the manufacturer's instruction. The extracted DNA was quantified by Nanodrop (Thermofisher) and the concentration was calculated per milligram of wet tissue mass. The size of the DNA fragments was assessed after electrophoresis in a 2% agarose gel containing SYBR safe (Thermofisher) for 1 h at 150 V. The gels were observed with iBright1500 (Thermo Fisher Scientific). GeneRuler 1 kb (Thermo Fisher Scientific) ladder was used for size control.

2.5. Scanning Electron Microscopy

Segments of native trachea, PDT and implanted PDT were fixed with Paraformaldehyde 2%, Glutaradaldehyde 2.5%, Sodium cacodylate 0.2 M pH 7.3. After washing in sodium cacodylate buffer, segments were cut into 0.25 cm^2 pieces, dehydrated through graded concentration of ethanol from 30% to 100%, critical point dried (CPD300, Leica), mounted on stubs and finally sputtered with 4 nm of platinum (ACE600, Leica). Scanning Electron Microscopy was conducted using a field emission gun Scanning Electron Microscope (GeminiSEM300, Carl Zeiss) with an acceleration voltage of 2 keV under high vacuum. Secondary electrons were collected. Scan speed and line averaging were adjusted during observation.

2.6. Biomechanical Properties

Compression testing was performed to evaluate the biomechanical properties of native trachea and PDT. The experiments were performed at 23 °C on a single-column, tabletop, universal testing machine (UTM) (model 5844; Instron Corp., Norwood, MA) equipped with a 2 kN load cell (Instron). Merlin Software (version 5.53.00; Instron) was used to control test execution and data collection. Four-ring specimens of native tracheas, cryopreserved native tracheas and PDT were equilibrated to room temperature and kept hydrated in PBS prior to testing. They were subjected to uniaxial radial compression testing by placement between two metal plates with the membranous side down. The upper plate was attached to the UTM load arm and lower plate was attached to the fixed UTM baseplate. Each specimen was compressed at a rate of 2.5 mm min^{-1} until 90% to 100% lumen occlusion was visible, at which point the test was stopped manually. Compressive load (N) versus compressive displacement (mm) data were obtained, and the load at 50% compressive displacement was calculated. Percentage of displacement was defined as Dx /D0×100, where Dx was the distance traveled, and D0 was the starting position.

2.7. Absence of Cytotoxicity of the PDT In Vitro

SDS Cytotoxic Threshold Concentration

Threshold cytotoxic concentration of SDS was defined on BALB/3T3 clone A31 cells (ATCC, U.S.A.), grown in DMEM (ATCC, U.S.A.) supplemented with 2% bovine calf serum (BCS, ATCC, Manassas, VA, USA) and 1% ATB/ATM. This cell line is recommended by European guidelines (Iso 109935-2009). BALB/3T3 cells were seeded at 1.5×10^4 cells $well^{-1}$ in a 48-well plate in a medium to which SDS had been added at a concentration ranging from 1% to 10^{-7}%. Positive controls were DMEM with 10% and 2% BCS. Negative control was culture medium containing 1% SDS.

After 48 h, cell viability was assessed after staining with LIVE/DEAD viability/cytotoxicity kit (Thermo-Fisher Scientific) containing calcein and ethidium homodimer-1. Images were acquired using a live microscope, Incucyte (Sartorius).

PDT Cytotoxicity on Balb/3T3 Cells

5-mm diameter samples of PDT were prepared with punches (Kai medical, Solingen, Germany) and incubated in 500 µL of Balb/3T3 culture medium containing 2% BCS. After 48 h, the supernatants were transferred on BALB/3T3 cells seeded at 1.5×10^4 cells $well^{-1}$ in a 48-well plate for 48 h. Cell viability was screened as described above, using the LIVE/DEAD viability/cytotoxicity kit with Incucyte (Sartorius).

Cell viability was also quantified by flow cytometry. At the end of the 48-h culture, floating cells in the supernatant were collected and the remaining cells were detached by a trypsin treatment. All cells were centrifuged and suspended in 1× apoptosis buffer (Invitrogen). They were stained with 2 µL $tube^{-1}$ Annexin V-FITC and 2 µL of Propidium iodide (PI) kit (Invitrogen). After 15 mins of staining at room temperature, cell viability was analyzed by flow cytometry, using an Attune-Nxt cytometer (Invitrogen, Thermo Fisher Scientific). Unstained cells were used as control for fluorescence. Viability positive controls were cells cultured in medium with 10% and with 2% BCS. Negative control was cells cultured in medium with 2% BCS containing 0.01% SDS. Annexin V^-/PI^- population was considered as viable.

Residual SDS Quantification

The concentration of residual SDS was measured by a spectrophotometric method, based on the use of a carbocyanine dye (Stains-all) the color of which changes from intense fuchsia to yellow upon addition of SDS. This method has been recently described by our team.[26] All microtiter assays were performed in a Dulbecco PBS buffer.

The absorbance was read at 450 nm, with a microplate reader « Varioskan Lux » (Thermo Scientific). Standards and samples analyzed are described below.

Standards Preparation

SDS concentration standards were prepared by dilution of the 20% stock solution in PBS, ranging from 0.01% to 0.00025% SDS and stored at room temperature. The linearity of the curve representing absorbance versus concentration was validated prior to the dosage. Simple linear regression was used for the validation of colorimetric standard curve.

SDS Adsorption Capacity of the Activated Charcoal Cartridge

First, the SDS adsorption capacity of the clinical-grade activated charcoal cartridge was validated using a 0,01% SDS solution, filtered in a closed circuit. Iterative samples were taken before starting the pump, then every hour for 4 h.

In order to evaluate the efficacy of each rinsing and detoxification step of the PDT, samples were taken from the decellularization solution (1% SDS initially), at the end of each rinsing (4 × 20mins), then at different time points, once the PDT were connected to the active charcoal cartridge.

SDS Released from PDT

Samples of PDT were lyophilized and stored at 4 °C. Samples of 30 mg were placed into 2 mL tubes with 1 mL of PBS. They were grinded with a Tissue Lyser (Qiagen) at 50 rpm for 15 mins and placed in an incubator for 48 h at 37 °C. Supernatants were collected and analyzed for the presence of SDS.

Seeding of the PDT with BEAS-2B Cell Line

Human bronchial epithelial cell line BEAS-2B (Merck) was seeded and amplified in SAGM Small Airway Epithelial Cell Growth Medium BulletKit (Lonza, USA), in collagen coated BioCoat flasks (Corning, USA). Once confluent, cells were detached by trypsin treatment and were suspended at a concentration of 4×10^6 cells mL^{-1}.

5-mm diameter punches of four different PDTs were prepared. Three punches/PDT were placed in ultra-low-fixation 24-well plates (Corning, USA). BEAS-2B were then added to the wells. The plates were placed on an agitator (Grantbio), in a cell culture incubator at 37 °C, 5% CO_2 for a week. Seeded PDT samples were fixed for 24 h in paraformaldehyde (PFA) 4%, included in paraffin and 5 µm thick sections were prepared. Samples were evaluated by histology. BEAS-2B adherence and distribution was assessed by HES staining.

2.8. In Vivo Vascularization and Biointegration in Pigs

2.8.1. Animal Care and Ethics Statement

Female hybrid Landrace, Large White and Pietrain pigs aged 4 months, weighing between 50 and 60 kg received a PDT graft. Female pigs were chosen over male ones for easier handling in the animal care facility, due to their calmer nature.

All experiments were performed in the same accredited animal facility. The experimental protocol was carried out in accordance with EU Directive 2010/63/EU and institutional guidelines for animal experiments. It was approved by the scientific committee of our institution, the ethics committee for animal experimentation n°INSERM-034, and the Ministry of National Education, Higher Education and Research (agreement number: project n°2 022 120 817 007 429 – V8 APAFiS # 42 094).

2.8.2. Anesthesia

All procedures were performed in sterile conditions in an operating room at the research facility of Laboratoire de Recherches Biochirurgicales de la Fondation Alain Carpentier [PARCCeINSERM], under general anesthesia after a fasting period of 24 h. The induction was performed by an injection of 4 mg kg^{-1} of propofol and 0.5 mg kg^{-1} of morphine hydrochloride intravenously. The animals were intubated and placed under controlled ventilation. Anesthesia was achieved by inhalation of 3 – 5% isoflurane in 100% oxygen, delivered at a rate of 1 L min^{-1}. A perfusion of Ringer's lactate was implemented at a rate of 10 – 20 mL kg^{-1} h^{-1}. Antibiotic prophylactic therapy was performed with an intravenous injection of 15 mg kg^{-1} cefamandole.

2.8.3. PDT Implantation in the Sterno-Cephalic Muscle

The skin was incised with a 15 cm median sagittal cervical incision. This approach enabled dissection of the sternocephalic muscle with preservation of the superior-anterior vascular pedicle and collaterals, and minimal dissection of the tracheal, thyroid and esophageal structures. Prior to implantation, the PDT was stented and stretched with a clinical-grade silicone stent (Rutter supra-stomal stent, Boston Medical Products, Shrewsbury, MA, USA). The stent was occluded on both sides. The PDT was then tensioned over the stent with two Ethibond 2/0 sutures (Ethicon, Johnson&Johnson France, 92 787 Issy-les-Moulineaux) at each end. The objectives of stenting were to avoid PDT retraction, proliferation of endoluminal fibroblasts and fluid sequestration, to avoid infection. The tensioning was intended to increase the contact surface of the inter-annular spaces with the recipient's muscle tissue, to promote neovascularization. The stented PDT was placed within the sterno-cephalic compartment. This compartment was sutured to itself using Vicryl 2/0 (Ethicon, Johnson&Johnson France, 92 787 Issy-les-Moulineaux). The white line was sutured with Vicryl 2/0. The skin was sutured in 3 plans with Vicryl 2/0. Antibiotic spray was applied to the skin scar. The scar was left open air for reasons of poor dressing tolerance and clinical monitoring.

2.8.4. PDT Explantation

After 28 days, the anesthetic procedures were similar. The previous incision was repeated and the PTD was harvested together with the adjacent muscle into which it had been revascularized. The native trachea was removed at the end of the procedure.

2.8.5. Local and Systemic Immune Response to the PDT

Local immune response induced by the PDT and vascularization were studied on deparaffinized histological sections. Immunohistology was performed with antibodies directed against CD3 (clone SP7; rabbit monoclonal antibody; Epredia Netherlands, Da Breda, NL), actin (clone 1A4, mouse monoclonal antibody; Agilent Dako, Agilent Technologies France, LES ULIS) and von Willebrand factor (rabbit polyclonal antibody; Agilent Dako). Native tracheas were used as control samples.

To study the systemic immune response, blood samples were taken during each general anesthesia: before implantation of the PDT (Day 0) and before explantation of the PDT (Day 28). K3-EDTA tubes (BD Vacutainer, ref 368 270, Becton Diskinson France, Rungis) were used for complete blood count, and tubes containing a separating gel and coagulation activator (BD Vacutainer, SST II Advance, ref 367 953, Becton Dickinson France, Rungis) were used to prepare serum samples for C-reactive protein (CRP) analysis.

Complete blood counts were performed by XN analyzers (Sysmex) and reviewed by a senior hematologist familiar with porcine blood cells.

Serum samples were prepared by centrifugation of the tubes at 3000 rpm. All samples were frozen at −80 °C before analysis. C reactive protein (CRP) was quantified by ELISA, using the Porcine C-Reactive Protein/CRP DuoSet ELISA kit (R&D systems), according to the manufacturer's instructions. Absorbance at 450 nm was measured using a VarioskanLux plate reader (Thermo scientific).

2.9. Statistical Analysis

Commercial computer statistical software (GraphPad Software Inc., USA) was used for statistical analysis. A p-value of less than 0.05 was considered to be statistically significant. Descriptive statistics are presented as column bars with mean and standard deviation.

Statistical tests for non-parametric distributions were used: Mann-Whitney test (DNA concentrations before and after decellularization and radial compression tests) and one-way ANOVA (cell viability). T-test was used for comparison of mean values in parametric distribution.

3. Results

3.1. Partial Decellularization Protocol was Effective

3.1.1. Sterility

All the tested tracheas were positive for bacterial and fungal growth before decontamination. Incubation with ATB/ATM removed all bacterial and fungal contamination. After the decellularization process, every sample was negative for bacterial and fungal presence (**Table 1**). After cryopreservation and thawing, no contamination was reported, neither bacterial nor fungal.

3.1.2. Histology

To assess the efficacy of the decellularization, histological examinations were performed on native tracheas, as well as on fresh and cryopreserved PDTs. HES staining showed that partial decellularization removed all cells and nuclei from the epithelium, the mucosa, the submucosal glands, the muscle and the blood vessels, but not from the tracheal cartilage, as expected (**Figure 2** and S1, Supporting Information). Picrosirius red (PSR) and Orcein staining demonstrated the preservation of collagen and elastic fibers respectively, after decellularization and after cryopreservation. Blue alcian staining demonstrated the retention of glycosaminoglycans (GAGs) within the cartilage after decellularization and cryopreservation (Figure 2).

3.1.3. DNA Quantification and Qualification in the Mucosa

The DNA content of the native tracheal mucosa was 344.8 ± 244.8 ng mg^{-1} and that of PDT mucosa was 33.42 ± 26.7 ng mg^{-1}. This corresponds to a 90.4% DNA elimination after decellularization (**Figure 3A**). DNA concentrations in the PDT were below 50 ng mg^{-1} and were therefore in accordance with Badylak's values for tissue decellularization standards.[27]

Furthermore, electrophoresis on agarose gel of the extracted DNA showed that in the native tracheas, DNA fragment size exceeded 1000 bp. In the PDT mucosa, no DNA fragments were visible (Figure 3B). This result is also in compliance with Badylak's decellularization recommendations.[27]

3.1.4. Scanning Electron Microscopy

Scanning electron microscopy (Figure 3C) of native tracheas showed the presence of a lining of ciliated epithelial cells and goblet cells within the lumen. As for the cartilage, as expected, it was composed of a dense ECM, embedding the chondrocytes. After decellularization, all epithelial cells were removed but chondrocyte debris were still present. As for the ECM, some disorganization of the fibers on the outer side of the PDT was visible. No visible damage was present in the cross-section of the cartilage, suggesting that the decellularization process does not negatively impact the cartilage ECM structure.

3.1.5. Biomechanical Properties

Cryopreserved and decellularized tracheal segments were less resistant to pressure compared to native tracheal segments, with a decrease from 3.36 ± 1.42 N (Native, n = 34) to 1.49 ± 0.37 N (cryopreserved native trachea, n = 8) and 0.88 ± 0.22 N (PDT, n = 9) (Figure 3D, Figure S2, Supporting Information). Nevertheless, we did not observe any spontaneous collapse in the PDT.

Table 1. Microbiological controls at different stages of the process.

Microbiological results at different stages of the process				
Samples	Before decontamination with antibiotics	After 24 h of decontamination with antibiotics	After decellularization/ before cryopreservation	After decellularization, cryopreservation and thawing
# 1	Positive	Negative	Negative	Negative
# 2	Positive	Negative	Negative	Negative
# 3	Positive	Negative	Negative	Negative
# 4	Positive	Negative	Negative	Negative

3.2. PDT was not Cytotoxic In Vitro

3.2.1. Preliminary Study of SDS Cytotoxic Concentration Threshold

Positive controls, corresponding to cells cultured in medium containing 10% or 2% BCS, showed a high viability (**Figure** 4A). The range of SDS dilutions on Balb/3T3 cells showed that they were alive for SDS-concentrations of 0.006% and below, corresponding to 60 ng mL^{-1}. At slightly higher concentrations (0007%), cell death was reproducible. This concentration of 0.006% was subsequently adopted as the cytotoxicity threshold of SDS.

3.2.2. Cytotoxicity of PDT on Balb/3T3 Cells

In live microscopy, the PDT supernatant was toxic on Balb/3T3 after 48 h of filtration on the charcoal cartridge, showing that SDS released from the PDT reached cytotoxic concentrations. After

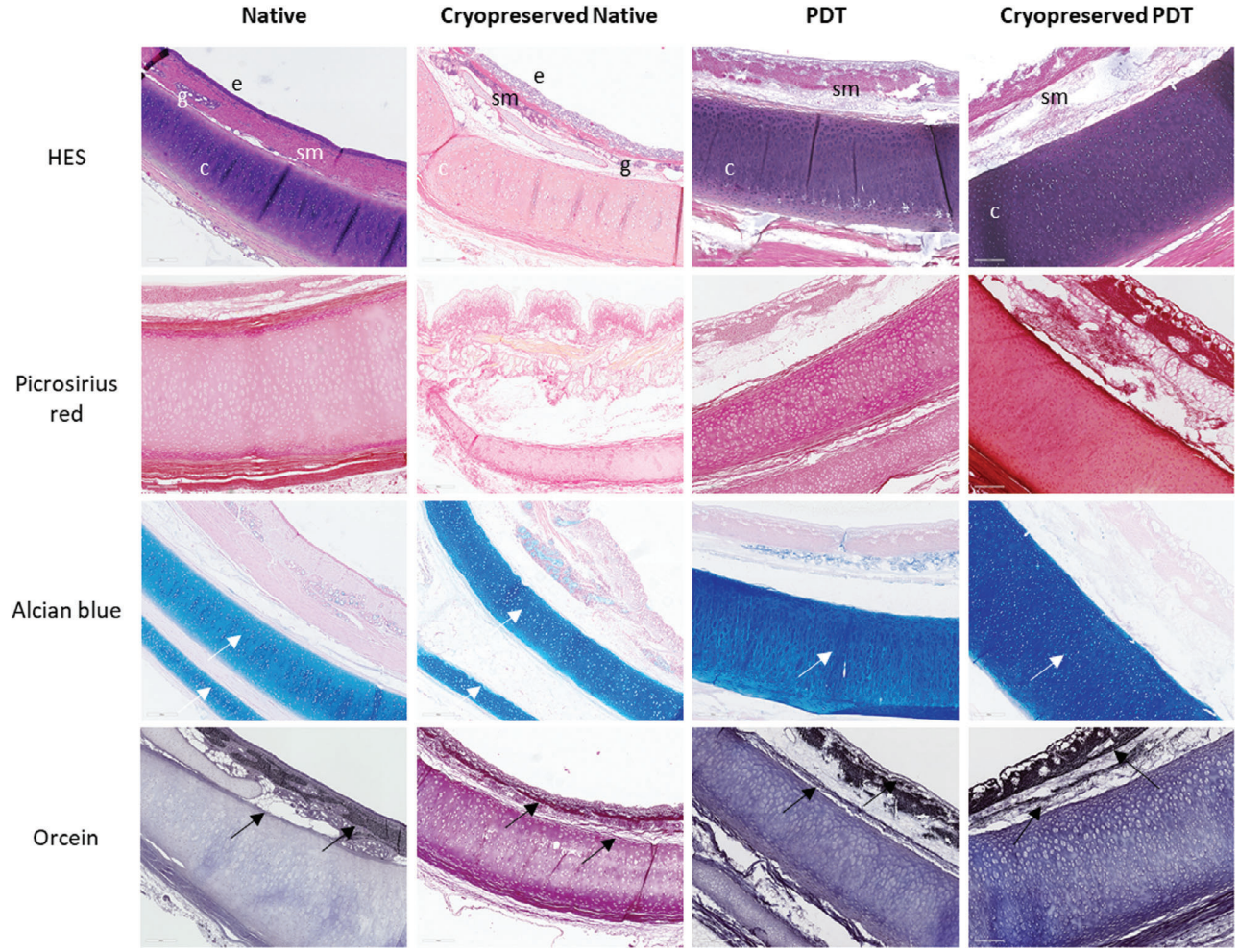

Figure 2. Histology of a porcine tracheas: Fresh Native trachea, Cryopreserved Native trachea, Partially Decellularized Trachea (PDT), and cryopreserved PDT are shown after staining with hematoxylin-eosin-saffron (HES) for the general structure, Picrosirius red for collagen, orcein for elastic fibers and Alcian Blue for glycosaminoglycans. Epithelium (e), sub-mucosa (sm), sub-mucosal gland (g) and cartilage (c) are shown in HES native trachea. Scale bars = 500 µm. PDT: Partially decellularized trachea. White arrows: elastic fibers, black arrow: glycosaminoglycans.

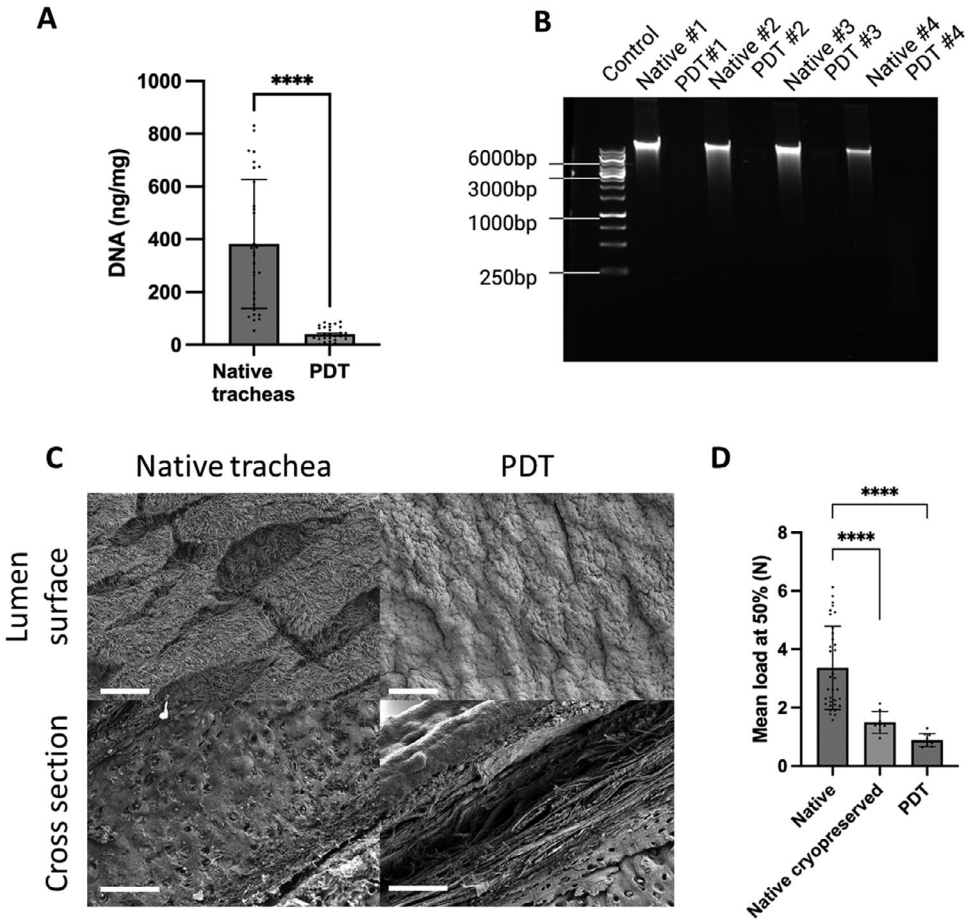

Figure 3. A) DNA quantity (ng mg^{-1} wet tissue) in native trachea and PDT mucosa. Donor matched tracheas were assessed and data were analyzed using a Mann-Whitney test (**** = $p < 0.0001$), n = 30. Mean DNA quantity in the native tracheas and PDT were 382.4 ± 244.8 ng mg^{-1} and 40.10 ± 26.76, respectively. B) DNA electrophoresis on agarose gel. DNA extracted from 30-mg mucosal sample of four matched tracheas were assessed, before and after decellularization. C) Scanning electron microscopy (SEM) images of the lumen surface and cross-section showing the cartilage of porcine native trachea and PDT samples. Scale bar = 50 µm. D) Radial compression of native tracheas, cryopreserved tracheas and PDT. Four-ring cartilage circular samples were compressed until occlusion. The results represent the mean force needed for 50% occlusion of the initial sample diameter (Mean load at 50%). Native tracheas: n = 34, mean: 3.364 ± 1.425 N; Native cryopreserved tracheas: n = 8, mean: 1.494 ± 0.3754 N; PDT: n = 9, mean: 0.8844 ± 0.2240. The statistical test Mann-Whitney was applied with a p value < 0.0001 for both comparisons of fresh native versus cryopreserved tracheas, and fresh native versus PDT.PDT: partially decellularized trachea.

96 h of detoxification, the PDT supernatant was not cytotoxic anymore and cells were alive (Figure 4B). These results were quantified by flow cytometry. At 96 h, the percentage of viable Balb/3T3 cells (Annexin V^-/ PI^-) cultured in the presence of PDT supernatant was not different than the control conditions, with a viability of 91.74 ± 2.35 with 10% CBS, 73.23 ± 9.92 with 2% CBS, 3.83 ± 1.08 with SDS 0.01% and 83.24 ± 7.14% with PDT supernatants (Figure 4C). These results demonstrated the absence of cytotoxicity induced by the PDT after the partial decellularization process.

3.2.3. BEAS-2B Epithelial Cell Seeding on PDT

Cell seeding with epithelial BEAS-2B cell line showed that these cells could adhere to the PDT, both to the cartilage and the connective tissue, and proliferate (Figure 4D). Comparison with the unseeded PDT patch, confirmed the absence of infiltration and colonization inside the cartilage. These results confirmed the biocompatibility of the PDT in vitro, by a direct method.

3.2.4. Residual SDS Quantification

The activated charcoal cartridge was effective at removing diluted SDS in water as there was no detectable SDS after 1 h of filtration (Figure 4E,F). Nevertheless, this rapid SDS elimination time corresponded to free SDS in a solution. Therefore, in order to evaluate the residual SDS trapped in the PDT, SDS quantification was performed directly on PDT rinsing supernatants. The first rinsing steps strongly eliminated the SDS but the levels remained above the cytotoxic threshold. Filtration on activated charcoal cartridge completely eliminated the SDS (Figure 4G). After 96 h of detoxification, no SDS could be detected in the tissue lysate supernatants obtained from PDT samples, showing an efficient removal of this detergent from tissues as well.

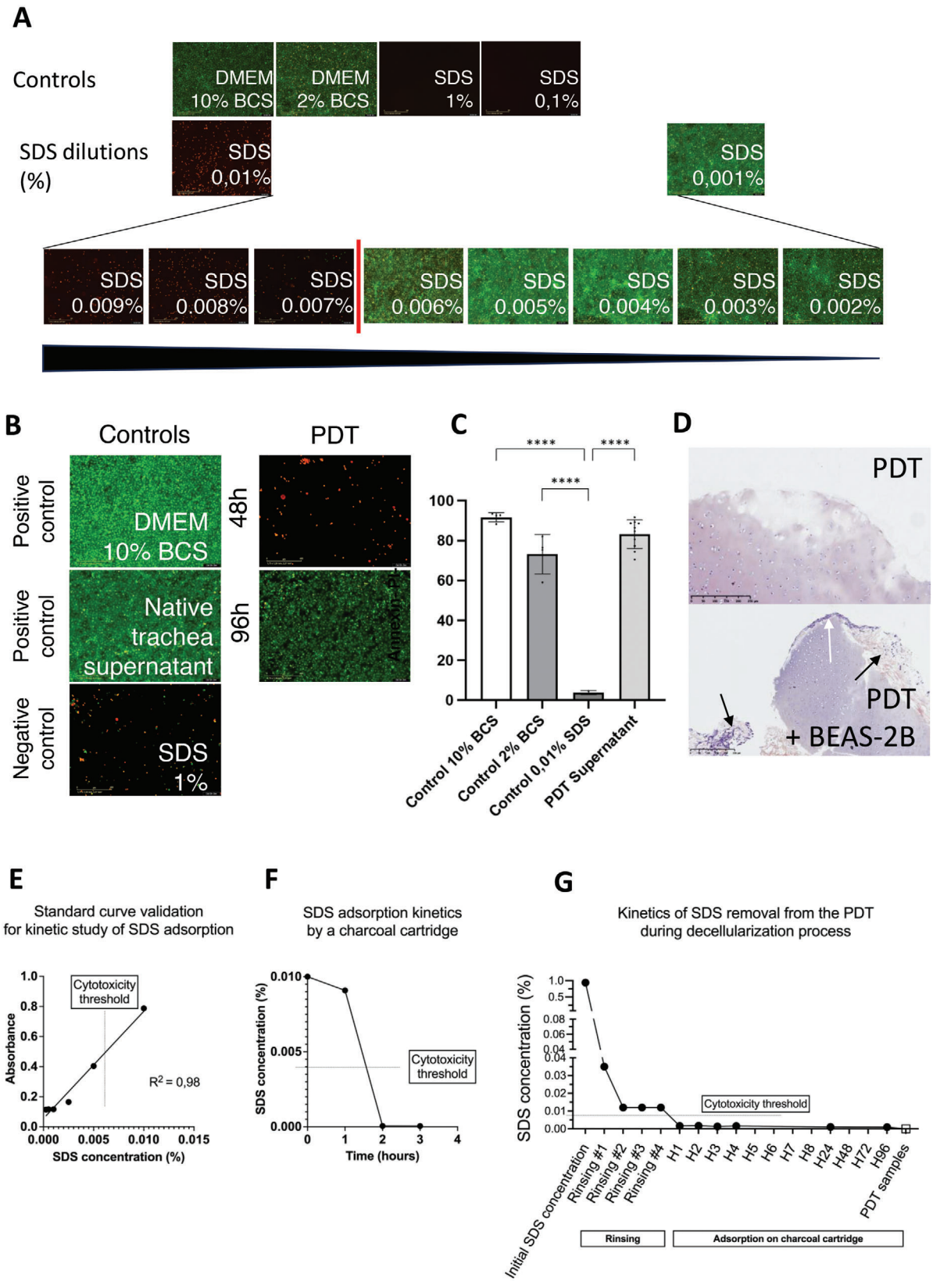

3.3. PDT was Biocompatible In Vivo

PDT were implanted in 3 pigs for 28 days. The pigs were monitored daily during this maturation period. No episodes of fever, general or local infection were reported. The pigs were in good health and showed no particular discomfort from the presence of the PDT or the scar.

Macroscopically, on excision, PDT were found within a typical fibrous gangue of a foreign-body reaction. There were no local signs of inflammation or infection, except for one pig which had a 1-cm subcutaneous abscess on a suture, not seen during clinical follow-up, with no extension to the implantation zone. After stent removal, the PDT was of satisfactory caliber, the cartilage rings were intact, there was no necrotic area. A rough test of the biomechanical properties was performed: to the touch, they appeared to have properties similar to those of native tracheas. They did not collapse and maintained their caliber over time (**Figure 5A**).

The length of the matured PDT was increased by an average of 23.5% due to the tension imposed during the maturation phase (Figure 5B). The purpose of this tension was to better expose the interannular ligaments to facilitate vascularization. The diameter, on the other hand, was reduced by an average of 24.5%. During maturation, the PDTs retracted around the 15-mm endoluminal stent.

3.3.1. Systemic Immune Response

Complete blood cell counts before PDT implantation (Day 0) and 28 days after implantation (Day 28) were compared (Figure 5C). On Day 28, there was no hyperleukocytosis or anemia. One pig had an isolated increase in platelets, with no clinical symptoms, except a centimetric CRP decreased during the implantation period, with no clinical evidence. The concentrations detected (D0: 6.9 mg L^{-1}, D28: 0.7 mg L^{-1}) remained within a physiological range[28,29] (Figure 5D).

3.3.2. Local Response and Tissue Remodeling

3.3.2.1. Vascularization: Vascularization was one of the main criteria of the biocompatibility of the PDT. It was therefore evaluated in vivo and histologically. To begin with, no necrosis of muscle surrounding the PTD was observed, showing the absence of toxicity and vascular erosion induced by the PDT. Furthermore, before euthanasia and explantation, small lesions were created in the implanted PDT to observe bleeding. This indeed resulted in the formation of blood droplets at these sites. In order to observe blood vessel formation within the PDT, histological sections of the implanted PDT were stained with vWF which identifies endothelial cells covering the newly formed blood vessels. This staining showed the presence of angiogenesis in the mucosa and adventice. The position of the newly formed vessels was comparable to the native trachea (**Figure 6A**).

3.3.2.2. Histology and Immune Cell Infiltration: HES staining showed that the overall architecture of the PDT was preserved. On all sections analyzed, the cartilaginous ECM was intact. There was neither cartilage, nor contact muscle lysis. The inner surface of the trachea was the site of a large fibrinous neo-tissue formation in the process of reorganization. Numerous cells had colonized the PDT (Figure 6A, HES and HES insert). This neoformed tissue was also observed in the external tunica of the trachea where it distended the intercartilaginous spaces. Picrosirius red showed the preservation of collagen. Orcein stained elastic fibers were still present in the submucosal site. GAGs were also highly preserved, mainly in the cartilage, as expected (Figure 6A). Immunostaining of actin showed that infiltrating cells are mainly myofibroblasts, participating to the scar tissue formation. No massive lymphocyte infiltration was detected in the PDTs and only a few $CD3^+$ cells were visible in the submucosal space. This was comparable to the native trachea, showing no signs of graft rejection. Neovascularization was confirmed by a large number of endothelial cells, labeled with the anti-vWF antibody (Figure 6B).

3.3.3. Scanning Electron Microscopy

The structure of the PDT was preserved after a 28-day maturation period in the muscle (Figure 6C). On the cross sections, the cartilaginous ECM seemed intact and well conserved. No major damage was observed on the basal lamina. Signs of bio-integration were evident and numerous cells colonized the lumen. These data confirmed the histological observations.

Figure 4. In vitro cytotoxicity study. A) Viability of BALB/3T3 was assessed with decreasing concentrations of Sodium dodecylsulfate (SDS), ranging from 0.01% to 0.001%. Positive controls were cells cultured in Dulbecco's Modified Eagle Medium (DMEM) with 10%, 2% calf bovine serum (CBS) and the negative control was cells treated with 1% SDS. Fluorescence was assessed after a 48-h treatment with various SDS concentrations. Green and red fluorescence were obtained by staining with LIVE/DEAD viability/cytotoxicity kit. Green (calcein) represents cell viability and red (ethidium homodimer-1) represents cell death. The viability threshold is shown with a red line. Experiments were performed in duplicate. B) Viability of BALB/3T3 was evaluated in the presence of partially decellularized tracheas (PDT) supernatants, collected at two different time points during detoxification (48 and 96 h). Cell culture media for positive and negative controls were Dulbecco's Modified Eagle Medium (DMEM) 10%, native trachea supernatant after decontamination, and SDS 1%, respectively (n = 15). C) BALB/3T3 cell viability in the presence of PDT supernatant, analyzed by flow cytometry. Cells were cultured for 48 h in control cell culture media: Bovine Calf Serum (BCS) 10% (n = 4), BCS 2% (n = 4) as positive controls and SDS 0.01% (n = 2) as negative control. Cell viability with PDT supernatants (n = 10) were evaluated. Percentage of Annexin-V^-/PI^- is represented. Mean viability percentages were: BCS 10%: 91.74 ± 2.35; BCS 2%: 73.23 ± 9.923; SDS 0.01%: 3.83 ± 1.08; PDT supernatants: 83.24 ± 7.14. Data were analyzed using one-way ANOVA (**** = $p < 0.0001$). D) Hematoxylin and eosin-saffron (HES) staining of PDT alone, and PDT seeded with BEAS cells. BEAS attached to perichondrium (white arrow). BEAS in conjunctive tissue (black arrow). Scale bars = 250 μm. E) Calibration measures of colorimetric dosage of SDS. A standard range of SDS concentrations (triplicates) was used to validate a standard curve and the reliability of the measurements. Cytoxicity threshold is represented, as found in (A). F) Adsorption of SDS by the charcoal cartridge. H0 SDS concentration was 0.01% and with a strong staining. From H1 onward, absorbance measurements were below the instrument's detection limit. G) SDS quantified in the decellularization supernatant of the PDT, at different timepoints of the protocol: beginning of the decellularization (initial SDS solution), after the four rinsing steps, and at different time points after filtration on activated charcoal cartridge (n = 1). PDT samples: SDS released from 30-mg PDT tissue lysates (n = 4).

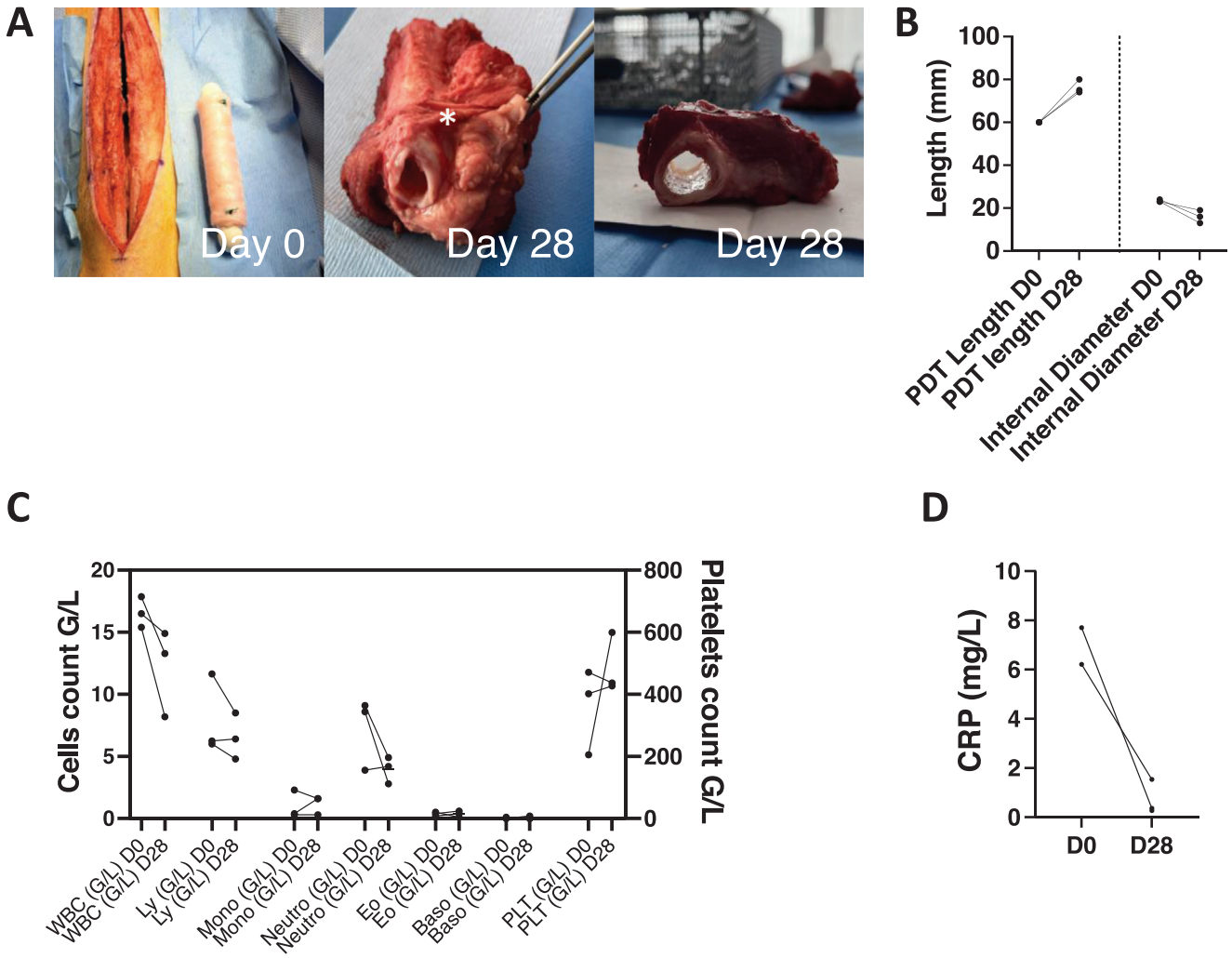

Figure 5. In vivo maturation of PDT. A) The macroscopic aspect of the partially decellularized trachea (PDT) is shown before implantation and after implantation after 28 days. Before implantation (Day 0), two of the four tension knots are visible (blue points). After 28 days of maturation (Day 28), PDT was explanted with the surrounding tissue: top view, scar tissue is seen between PDT and sterno-cephalic muscle (white asterisk). In the lateral view, there was no collapse and no inflammation inside the implanted PDT. B) Representation of changes in length and internal diameter of the trachea during implantation in a muscle. Measurements were taken at the time of implantation, then after explantation and stent removal. C) Evolution of white blood cells (WBC), lymphocytes (Ly), monocytes (Mono), granulocytes neutrophils (Neutro), Eosinophiles (eosino), basophils (baso), and platelets (PLT) during implantation. D) C-Reactive Protein dosage at implantation (Day 0) and explantation (Day 28).

Collagen II, Laminin and DAPI Staining

For a detailed evaluation of ECM remodeling, a comparative study on the native trachea, PDT before implantation, and PDT after 28 days of implantation in the muscle was performed. Collagen II and laminin staining showed that most of these ECM proteins in the native trachea were found within the mucosa and the submucosa. In the PDT, some of these proteins and their structure were lost, partly by an edema induced during decellularization. In the implanted PDT, these proteins were preserved and were reorganized. The edema was also absorbed (Figure 6D).

In the native trachea, DAPI showed a dense staining within the compact epithelium. Less dense but strongly present nuclear staining was observed in the submucosa and in the cartilage. In comparison, in the PDT, no DAPI staining was observed in the mucosa and the submucosa, while within the cartilage, cell nuclei could be found, confirming an efficient partial decellularization (Figure 6D, Figure S3, Supporting Information). In the implanted PDT, a strong DAPI staining was observed, especially within the submucosa (Figure 6D), confirming cell infiltration.

4. Discussion

Partial decellularization of the tracheal substitute was described by Liu in 2000[17,18] and still is an active field of research. Indeed, tracheal epithelium presents a strong immunogenicity and is the first target of graft rejection[30] whereas the chondrocytes are much less immunogenic. Therefore, partial decellularization, focusing on the removal of epithelial and mucosal cells, while preserving cartilage structure, prevents graft rejection, as well as an obstruction of the tracheal lumen through the preservation of optimal biomechanical properties.[22,31]

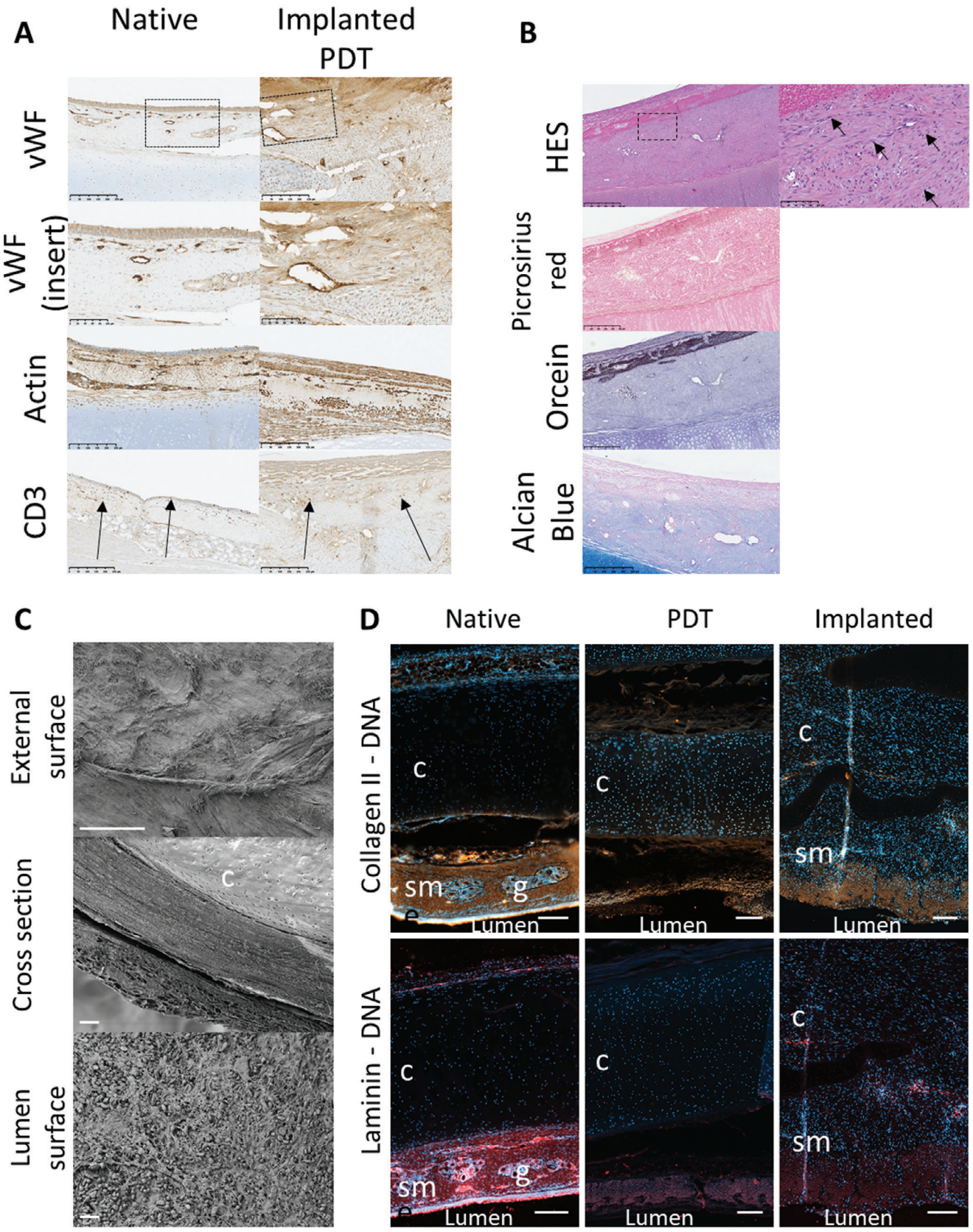

Most tracheal decellularization protocols described in the literature remain research grade, with limited characterization of the final product's sterility, cytotoxicity and translational potential. The only clinical tracheal reconstructions with decellularized tracheas, in compassionate use, applied a protocol of full decellularization that took 3 weeks to prepare, with 25 cycles of detergent enzymatic treatment[14] which most probably impaired cartilage biomechanical properties. The biochemical and biomechanical characteristics, as well as residual detergent levels were not described.[15] In a translational perspective of the development of a standardized clinical grade protocol, we chose to optimize the animal model, the decellularization protocol and products. Furthermore, a number of systemic and local immunological responses to the PDT were studied.

To begin with, we chose a tracheal anatomical model as close to humans as possible. The pig has a tracheal size and shape similar to humans and is more relevant compared to smaller models such as mice. Furthermore, the pig has a closer immune system to humans. Therefore, this model presents an advantage in understanding the biointegration mechanisms in vivo.[25] For these reasons, we chose to develop our decellularization protocol, as well as the re-implantation in a porcine model.

We propose hereby a clinically relevant protocol for partial tracheal decellularization that removes endotracheal epithelial cells and submucosal cells. To ensure the clinical translational potential of our protocol, we adhered as much as possible to clinical standards of Cell and Tissue products. This included the use of medical grade products such as Pulmozyme and medical grade activated charcoal cartridge, previously used by our team for the development of a clinical grade decellularized esophagus.[26] Particular attention was paid to sterility, and an extended quality control including histology, cytotoxicity, and in vitro and in vivo biocompatibility. Most importantly, the results were reproducible, demonstrating the reliability of the procedure.

Since our aim was to achieve decellularization of the mucosa and submucosa, we increased the SDS treatment time compared with Aoki's protocol,[21] which still retrieved cells and DNA in the submucosa after 3-h SDS exposure and could lead to anti-inflammatory response linked to imperfect decellularization. This treatment fully removed the cells and their genetic materials from the mucosa and submucosa, confirmed by histology and DAPI staining. On the other hand, cell nuclei could be found in the cartilage, as expected. We believe that after resection and the decellularization procedure, no viable chondrocytes remain in the cartilage. However, the presence of cell nuclei in this compartment shows that detergent infiltration is limited, reducing the damage to the cartilage ECM. This is important for maintaining the biomechanical properties of the PDT.

For future clinical use, a cryopreservation protocol was developed in order to prepare a bank of PDT. For the cryopreservation medium, we used RPMI supplemented with 10% DMSO and 0.8% albumin. This medium is used in routine for the cryopreservation of aorta, as well as clinical grade decellularized esophagi by the human Tissue Bank of the AP-HP.[26] Our protocol consisted of an overnight freezing at −20 °C, followed by a long-term storage at −80 ° C. This protocol allowed preserving the general structure of the trachea and the sterility. However, the mechanical testing showed that cryopreservation partially compromised the biomechanical properties. These results were comparable to the PDT. Even though in histology, no major damage was observed in cryopreserved tracheas, the loss of rigidity could be linked to microfractures that could not be observed by this method. Furthermore, this could be explained by a loss of contractile muscles after cryopreservation and decellularization, that intervene in the biomechanical properties of the trachea.[32] To reduce the effect of cryopreservation, a new protocol including a controlled temperature drop is currently being tested. Quick cooling by a vitrification procedure could be an interesting alternative technique.[33,34]

To evaluate in vivo biointegration, we decided to implant the PDT in the sterno-cephalic muscle. Indeed, like other decellularized tissues, the PDT first needs to be revascularized within the recipient organism (heterotopic graft) before orthotopic replacement. This neovascularization can be achieved by grafting the decellularized tissues in a muscle, the grand omentum or a skin flap. In large animals, this two-stage process is widely accepted.[35–38] The same procedure has also been used in humans by Delaere.[20] During the maturation phase, the PDT, which is not yet vascularized, is stented to avoid the formation of a collection and to prevent it from retracting. In our in vivo study, we used a similar approach, by maturing the PDT in a muscle compartment for 28 days. The results were promising, showing an efficient neo-vascularization and biointegration without signs of rejection. Especially, no extensive local lymphocyte infiltration was seen. Moreover, no biological sign of graft rejection was noticed.

Contrary to the study by Haykal et al.[39] but in line with our previous work,[40] we did not add MSC during the implantation phase. MSCs have not been shown to improve the biointegration of a decellularized esophageal matrix, nor have they been shown to improve immunomodulation. On the other hand, we believe that recellularization with autologous epithelial cells could be highly beneficial for limiting fibroblast and lymphocyte proliferation, as well as for preventing infection through a muco-ciliary barrier.[41,42]

In consideration of a future clinical application, it is also important to apply the regulatory constraints of production required by health authorities. If used alone, the PDT can fall into the category of Cell and Tissue (CT) products. If cells are expanded in vitro and reseeded on PDT, the combined product becomes an Advanced Therapy Medicinal Product. In both cases, the final PDT should be produced in a specific GMP facility, with extensive quality control criteria. In order to facilitate future technology

Figure 6. Immune and inflammatory response to implantation. A) Comparison of immunostaining between native trachea and reimplanted PDT with anti Von Willebrand Factor (vWF), Actin and CD3 antibodies. $CD3^+$ cells are shown with black arrows. Scale bar = 250 μm, except insert, scale bar = 100 μm. B) Histological studies of a partially decellularized trachea (PDT) after 28 days of muscular implantation are shown using hematoxylin-eosin-saffron (HES) for the general structure, Picrosirius red (PSR) for collagen, orcein for elastic fibers and Alcian blue for glycosaminoglycan staining. Scale bar = 500 μm, except insert 100 μm. C) Scanning electron microscopy (SEM) images of external surface, cross-section and lumen surface of implanted PDT sample. Scale bar = 100 μm. D) Immunofluorescence of native trachea and PDT with anti-collagen II (orange) and laminin (red) antibodies. Scale bar = 200 μm.

transfer to a clinical grade production facility, we worked in strong collaboration with the human tissue bank throughout the whole process. Our team has shown a similar approach in the development of clinical grade decellularized esophagi as well[26] which is currently being evaluated for a phase I/II clinical trial.

Furthermore, it is important to evaluate the efficiency of the clinical grade PDT in vivo, in a large animal model by a long-term follow-up, in order to have a clearer view of biointegration and the immune response. The next step is also to evaluate the efficacy of the PDT implanted in an orthotopic position, for a circumferential replacement of the trachea.

5. Conclusion

Despite a large number of reported studies on the development of decellularized tracheal protocols, most of them remain research grade, with limited characterization of the final product, mainly its sterility and toxicity. We hereby report a reliable and reproducible clinical grade PDT. The first in vivo results showed an excellent biointegration in a heterotopic position. These results are promising and will be pursued for the replacement of a circumferential tracheal replacement. The ultimate goal of this project is the development of a clinical trial.

Supporting Information

Supporting Information is available from the Wiley Online Library or from the author.

Acknowledgements

The authors disclosed receipt of the following financial support for the research, authorship, and/or publication of this article: the authors acknowledge technical support from animal care and veterinary staff and Julie Piquet at the Biosurgical research laboratory of Fondation Carpentier. The authors also thank INRAe (French National Research Institute for Agriculture, Food and the Environment) and Sylvain Bourgeais for their technical support and supply. The authors would like to thank Dr. Elisa Peroni and Dr. Olivier Monasson from BioCIS laboratory for the development of the SDS quantification method. This work was supported by the Institut National de la Santé et de la Recherche Médicale (grant number EN_2020CINT05), l'Assistance publique – Hôpitaux de Paris (AP-HP), Fondation de l'Avenir pour la Recherche Médicale Appliquée (grant number APRM19-007), Agence de la Biomédecine (grant number 20Greffe011), and Association Française de l'Atrésie de l'Œsophage. None of the funders were involved in carrying out the research or writing up the results.

Conflict of Interest

A European patent has been filed under number EP23306699.2. The declared inventors are Briac Thierry, Lousineh Arakelian, Valentino Caputo and Jérôme Larghero. The author(s) declare no further conflict of interest.

Author Contributions

B.T., L.A. Conceptualization; B.T., L.A. Methodology; B.T. J.M.A, V.C. Software; B.T., M.L., V.C., R.G., R.B., L.A. Validation; B.T., J.M.A., V.C. Formal analysis; B.T., M.L., V.C., A.V. Investigation; S.K., R.A., P.B., J.M.A, N.G., C.S., M.J. A.V. Resources; B.T. Data curation ; B.T., L.A. Writing – original draft; B.T., L.A., S.K., R.A., J.L. Writing – Review & Editing; B.T., R.G. Visualization ; F.D., J.L. Supervision ; B.T. Project administration; B.T., J.L. Funding acquisition.

Data Availability Statement

The data that support the findings of this study are available from the corresponding author upon reasonable request.

Keywords

biointegration, clinical grade, partial decellularization, trachea, vascularization

Received: April 16, 2024
Revised: July 9, 2024
Published online: August 20, 2024

[1] H. C. Grillo, *Thorax* **1973**, *28*, 667.
[2] D. Fabre, F. Kolb, E. Fadel, O. Mercier, S. Mussot, T. L. Chevalier, P. Dartevelle, *Ann. Thorac. Surg.* **2013**, *96*, 1146.
[3] F. Kolb, F. Simon, R. Gaudin, B. Thierry, S. Mussot, L. Dupic, J.-L. Coste, N. Leboulanger, F. Denoyelle, V. Couloigner, E.-N. Garabedian, *N. Engl. J. Med.* **2018**, *378*, 1355.
[4] T. Kubo, T. Kurita, H. Tashima, M. Suzuki, H. Uemura, T. Fujii, S. Seike, H. Inohara, K. Hosokawa, *Microsurgery* **2018**, *39*, 46.
[5] C. Thomet, A. Modarressi, E. M. Rüegg, P. Dulguerov, B. Pittet-Cuénod, *Ann. Plast. Surg.* **2018**, *1*, 525.
[6] E. M. Genden, B. A. Miles, T. J. Harkin, S. DeMaria, A. J. Kaufman, E. Mayland, V. F. Kaul, S. S. Florman, *Am. J. Transplant.* **2021**, *21*, 3421.
[7] V. D. Parshin, A. V. Lyundup, E. A. Tarabrin, V. V. Parshin, *Khirurgiia (Mosk)* **2018**, *11*, 11.
[8] A. M. Greaney, L. E. Niklason, *Tissue Eng. Part B* **2021**, *27*, 341.
[9] R. Kaye, T. Goldstein, D. A. Grande, D. Zeltsman, L. P. Smith, *Int. J. Pediatr. Otorhinolaryngol.* **2019**, *117*, 175.
[10] J.-H. Park, J.-K. Yoon, J. B. Lee, Y. M. Shin, K.-W. Lee, S.-W. Bae, J. Lee, J. Yu, C.-R. Jung, Y.-N. Youn, H.-Y. Kim, D.-H. Kim, *Sci. Rep.* **2019**, *9*, 2103.
[11] E. Martinod, K. Chouahnia, D. M. Radu, P. Joudiou, Y. Uzunhan, M. Bensidhoum, A. M. Santos Portela, P. Guiraudet, M. Peretti, M.-D. Destable, A. Solis, S. Benachi, A. Fialaire-Legendre, H. Rouard, T. Collon, J. Piquet, S. Leroy, N. Vénissac, J. Santini, C. Tresallet, H. Dutau, G. Sebbane, Y. Cohen, S. Beloucif, A. C. d'Audiffret, H. Petite, D. Valeyre, A. Carpentier, E. Vicaut, *JAMA, J. Am. Med. Assoc.* **2018**, *319*, 2212.
[12] A. Wurtz, H. Porte, M. Conti, J. Desbordes, M.-C. Copin, J. Azorin, E. Martinod, C.-H. Marquette, *N. Engl. J. Med.* **2006**, *355*, 1938.
[13] A. Wurtz, H. Porte, M. Conti, C. Dusson, J. Desbordes, M.-C. Copin, C.-H. Marquette, *J. Thorac. Cardiovasc. Surg.* **2010**, *140*, 387.
[14] M. J. Elliott, P. De Coppi, S. Speggiorin, D. Roebuck, C. R. Butler, E. Samuel, C. Crowley, C. McLaren, A. Fierens, D. Vondrys, *Lancet* **2012**, *380*, 994.
[15] M. J. Elliott, C. R. Butler, A. Varanou-Jenkins, L. Partington, C. Carvalho, E. Samuel, C. Crowley, P. Lange, N. J. Hamilton, R. E. Hynds, T. Ansari, P. Sibbons, A. Fierens, C. McLaren, D. Roebuck, C. Wallis, N. Muthialu, R. Hewitt, D. Crabbe, S. M. Janes, P. De Coppi, M. W. Lowdell, M. A. Birchall, *Stem Cells Transl. Med.* **2017**, *6*, 1458.
[16] E. J. Culme-Seymour, K. Mason, L. Vallejo-Torres, C. Carvalho, L. Partington, C. Crowley, N. J. Hamilton, E. C. Toll, C. R. Butler, M. J. Elliott, M. A. Birchall, M. W. Lowdell, C. Mason, *Tissue Eng., Part A* **2016**, *22*, 208.
[17] Y. Liu, T. Nakamura, Y. Yamamoto, K. Matsumoto, T. Sekine, H. Ueda, Y. Shimizu, *J. Thorac. Cardiovasc. Surg.* **2000**, *120*, 108.
[18] Y. Liu, T. Nakamura, Y. Yamamoto, K. Matsumoto, T. Sekine, H. Ueda, Y. Shimizu, *ASAIO J.* **2000**, *46*, 536.

[19] Y. Liu, T. Nakamura, Y. Shimizu, H. Ueda, M. Yoshitani, T. Toba, S. Fukuda, *Ann. Thorac. Surg.* **2001**, *72*, 1190.
[20] P. Delaere, J. Vranckx, G. Verleden, P. De Leyn, D. Van Raemdonck, *N. Engl. J. Med.* **2010**, *362*, 138.
[21] F. G. Aoki, R. Varma, A. E. Marin-Araujo, H. Lee, J. P. Soleas, A. H. Li, K. Soon, D. Romero, H. T. Moriya, S. Haykal, C. Amon, T. K. Waddell, G. Karoubi, *Sci. Rep.* **2019**, *9*, 12034.
[22] L. Liu, S. Dharmadhikari, K. M. Shontz, Z. H. Tan, B. M. Spector, B. Stephens, M. Bergman, A. Manning, K. Zhao, S. D. Reynolds, C. K. Breuer, T. Chiang, *J Tissue Eng* **2021**, *12*, 204173142110174.
[23] D. Rana, H. Zreiqat, N. Benkirane-Jessel, S. Ramakrishna, M. Ramalingam, *J. Tissue Eng. Regener. Med.* **2017**, *11*, 942.
[24] M. Kasravi, A. Ahmadi, A. Babajani, R. Mazloomnejad, M. R. Hatamnejad, S. Shariatzadeh, S. Bahrami, H. Niknejad, *Biomater. Res.* **2023**, *27*, 10.
[25] R. Pabst, *Cell Tissue Res.* **2020**, *380*, 287.
[26] W. Godefroy, L. Faivre, C. Sansac, B. Thierry, J.-M. Allain, P. Bruneval, R. Agniel, S. Kellouche, O. Monasson, E. Peroni, M. Jarraya, N. Setterblad, M. Braik, B. Even, S. Cheverry, T. Domet, P. Albanese, J. Larghero, P. Cattan, L. Arakelian, *Sci. Rep.* **2023**, *13*, 18283.
[27] S. F. Badylak, D. Taylor, K. Uygun, *Annu. Rev. Biomed. Eng.* **2011**, *13*, 27.
[28] I. Hennig-Pauka, A. Menzel, T. R. Boehme, H. Schierbaum, M. Ganter, J. Schulz, *Vet. Sci.* **2019**, *6*, 92.
[29] C. Velik-Salchner, C. Schnürer, D. Fries, P. R. Müssigang, P. L. Moser, W. Streif, C. Kolbitsch, I. H. Lorenz, *Thromb. Res.* **2006**, *117*, 597.
[30] E. Kuo, A. Bharat, J. Shih, T. Street, J. Norris, W. Liu, W. Parks, M. Walter, G. A. Patterson, T. Mohanakumar, *Ann. Thorac. Surg.* **2006**, *82*, 1226.
[31] L. Liu, S. Dharmadhikari, B. M. Spector, Z. H. Tan, C. E. Van Curen, R. Agarwal, S. Nyirjesy, K. Shontz, S. A. Sperber, C. K. Breuer, K. Zhao, S. D. Reynolds, A. Manning, K. K. VanKoevering, T. Chiang, *J. Tissue Eng.* **2022**, *13*, 204173142211087.
[32] R. Kaye, A. Cao, T. Goldstein, D. A. Grande, D. Zeltsman, L. P. Smith, *Am. J. Otolaryngol.* **2022**, *43*, 103217.
[33] P. Mallis, M. Katsimpoulas, A. Kostakis, D. Dipresa, S. Korossis, A. Papapanagiotou, E. Kassi, C. Stavropoulos-Giokas, E. Michalopoulos, *Tissue Eng. Regen. Med.* **2020**, *17*, 285.
[34] J. Bakhach, *Organogenesis* **2009**, *5*, 119.
[35] W. Klepetko, G. M. Marta, W. Wisser, E. Melis, A. Kocher, G. Seebacher, C. Aigner, S. Mazhar, *J. Thorac. Cardiovasc. Surg.* **2004**, *127*, 862.
[36] T. Jana, E. Khabbaz, C. M. Bush, J. D. Prosser, M. A. Birchall, C. A. Nichols, G. N. Postma, P. M. Weinberger, *Eur. Arch. Otorhinolaryngol.* **2013**, *270*, 181.
[37] M. Den Hondt, B. M. Vanaudenaerde, E. K. Verbeken, J. J. Vranckx, *Interact. Cardiovasc. Thorac. Surg.* **2018**, *26*, 753.
[38] I. V. Gilevich, A. S. Sotnichenko, D. D. Karal-ogly, E. A. Gubareva, E. V. Kuevda, I. S. Polyakov, B. A. Lapin, S. V. Orlov, V. A. Porkhanov, V. P. Chekhonin, *Bull. Exp. Biol. Med.* **2018**, *164*, 770.
[39] S. Haykal, Y. Zhou, P. Marcus, M. Salna, T. Machuca, S. O. P. Hofer, T. K. Waddell, *Biomaterials* **2013**, *34*, 5821.
[40] G. Levenson, A. Berger, J. Demma, G. Perrod, T. Domet, L. Arakelian, P. Bruneval, C. Broudin, M. Jarraya, N. Setterblad, G. Rahmi, J. Larghero, P. Cattan, L. Faivre, T. Poghosyan, *Surgery* **2022**, *171*, 384.
[41] R. J. Hewitt, C. M. Lloyd, *Nat. Rev. Immunol.* **2021**, *21*, 347.
[42] E. F. Maughan, R. E. Hynds, T. J. Proctor, S. M. Janes, M. Elliott, M. A. Birchall, M. W. Lowdell, P. De Coppi, *Curr. Stem Cell Rep.* **2017**, *3*, 279.